

Quasistatic cloaking of two-dimensional polarizable discrete systems by anomalous resonance

Nicolae-Alexandru P. Nicorovici¹, Graeme W. Milton²,
Ross C. McPhedran^{1*}, and Lindsay C. Botten³

¹*CUDOS, School of Physics, University of Sydney, NSW 2006, Australia*

²*Department of Mathematics, University of Utah, Salt Lake City, Utah 84112, USA*

³*CUDOS, Department of Mathematical Sciences, University of Technology, Sydney, NSW 2007, Australia*

ross@physics.usyd.edu.au

Abstract: Discrete systems of infinitely long polarizable line dipoles are considered in the quasistatic limit, interacting with a two-dimensional cloaking system consisting of a hollow plasmonic cylindrical shell. A numerical procedure is described for accurately calculating electromagnetic fields arising in the quasistatic limit, for the case when the relative permittivity of the cloaking shell has a very small imaginary part. Animations are given which illustrate cloaking of discrete systems, both for the case of induced dipoles and induced quadrupoles on the interacting particles. The simulations clarify the physical mechanism for the cloaking.

© 2007 Optical Society of America

OCIS codes: (160.4760) Optical properties; (260.2110) Electromagnetic theory; (260.5740) Resonance; (350.7420) Waves

References and links

1. J. B. Pendry, D. Schurig, and D. R. Smith, "Controlling electromagnetic fields," *Science* **312**, 1780–1782 (2006).
2. U. Leonhardt, "Optical conformal mapping," *Science* **312**, 1777–1780 (2006).
3. D. Schurig, J. J. Mock, B. J. Justice, S. A. Cummer, J. B. Pendry, A. F. Starr, and D. R. Smith, "Metamaterial Electromagnetic Cloak at Microwave Frequencies," *Science* **314**, 977–980 (2006).
4. A. Greenleaf, M. Lassas, and G. Uhlmann, "Anisotropic conductivities that cannot be detected by EIT," *Physiol. Meas.* **24** 413–419 (2003).
5. A. Greenleaf, Y. Kurylev, M. Lassas, and G. Uhlmann, "Full-wave invisibility of active devices at all frequencies," <http://arxiv.org/abs/math.AP/0611185>.
6. G. W. Milton, M. Briane, and J. R. Willis, "On cloaking for elasticity and physical equations with a transformation invariant form," *New J. Phys.* **8**, 248–267 (2006).
7. W. Cai, U. K. Chettiar, A. V. Kildishev, and V. M. Shalaev, "Optical Cloaking with Non-Magnetic Metamaterials," <http://arxiv.org/pdf/physics/0611242>.
8. N. A. Nicorovici, R. C. McPhedran, and G. W. Milton, "Optical and dielectric properties of partially resonant composites," *Phys. Rev. B* **49**, 8479–8482 (1994).
9. T. J. Cui, Q. Cheng, W. B. Lu, Q. Jiang, J. A. Kong, "Localization of electromagnetic energy using a left-handed-medium slab," *Phys. Rev. B* **71**, 045114 (2005).
10. A. D. Boardman and K. Marinov, "Non-radiating and radiating configurations driven by left-handed metamaterials," *J. Opt. Soc. Am. B* **23**, 543–552 (2006).
11. V. A. Fedotov, P. L. Mladonov, S. L. Prosvirnin, and N. I. Zheludev, "Planar electromagnetic metamaterial with a fish scale structure," *Phys. Rev. E* **72**, 056613 (2005).
12. G. W. Milton, N.-A. P. Nicorovici, R. C. McPhedran, and V. A. Podolskiy, "A proof of superlensing in the quasistatic regime, and limitations of superlenses in this regime due to anomalous localized resonance," *Proc. R. Soc. Lond. A* **461**, 3999–4034 (2005).

13. G. W. Milton and N.-A. P. Nicorovici, "On the cloaking effects associated with anomalous localized resonance," *Proc. Roy. Soc. A* **462**, 3027–3059 (2006).
14. G. W. Milton, N.-A. P. Nicorovici, and R. C. McPhedran, "Opaque perfect lenses," *Physica B* **394**, 171–175 (2007).
15. M. Kerker, "Invisible bodies," *J. Opt. Soc. Am.* **65**, 376–379 (1975).
16. A. Alu and N. Engheta, "Pairing an epsilon-negative slab with a mu-negative slab: resonance, tunneling and transparency," *IEEE Trans. Antennas Propag.* **51**, 2558–2571 (2003).
17. A. Alu and N. Engheta, "Achieving transparency with plasmonic and metamaterial coatings," *Phys. Rev. E* **72**, 016623 (2005).
18. A. G. Ramm, "Invisible obstacles," *Ann. Polon. Math.* **90**, 145–148 (2007).
19. D. A. B. Miller, "On perfect cloaking," *Opt. Express* **14**, 12457–12466 (2006).
20. P. Sheng, "Waves on the horizon," *Science* **313**, 1399–1400 (2006).
21. P. Weiss, "Out of Sight: Physicists get serious about invisibility shields," *Science News* **170**, 42–44 (2006).
22. Supporting Online Material, <http://www.physics.usyd.edu.au/cudos/research/plasmon.html>.
23. O. P. Bruno and S. Lintner, "Superlens-cloaking of small dielectric bodies in the quasistatic regime," submitted.

1. Introduction

In recent years much interest has been aroused by the possibility of cloaking or hiding objects from interrogation by electromagnetic waves. Many schemes are under active current investigation. One of these, put forward by Pendry *et al.* [1] and Leonhardt [2], relies on surrounding the object to be cloaked by a metamaterial shell of varying structure, designed to afford appropriate effective optical properties to ensure light paths can be controlled. This structure guides light around a central hole, in which the object to be cloaked can be placed. Cloaking is successful in a range of frequencies in which the metamaterial structure has the required effective properties, with experimental evidence having been presented [3] for the effectiveness of this concept at microwave frequencies. Note that current experimental evidence for cloaking is restricted to two-dimensional systems and to quite narrow frequency ranges, with the extent of the cloaking being limited by as-yet unoptimized material properties. Other theoretical studies of cloaking by this mechanism have been made by Greenleaf *et al.* [4, 5], Milton *et al.* [6], and Cai *et al.* [7].

A second mechanism for cloaking relies on resonant interaction to mask the electromagnetic signature of the body to be cloaked. In contrast to the first method, which cloaks a body *internal* to the metamaterial structure, here the cloaking is achieved in a region *external* to the cloaking body. In a 1994 paper [8], we proved the existence of a transparency (zero reflectivity) property of a cylindrical perfect lens, which is similar to that which arises in a perfect slab lens where it is due to the mirroring property of a planar interface between media having opposite permittivities and permeabilities. This mirroring property led Cui *et al.* [9] and Boardman *et al.* [10] to realize that two appropriately placed sources, on opposite sides of a planar superlens, would cloak each other but trap an enormous field in the layer between them. The transparency of cylindrical lenses is also related to the existence of current sources (on the surface) that do not radiate [11]. Later on, in a more detailed analysis of the result of Refs [8, 12] we discovered [13, 14] the cloaking of infinitely long polarizable line dipoles (hereafter referred to as "polarizable line dipoles" in the interest of brevity) by *anomalous resonances*. An inhomogeneous body with piecewise constant moduli exhibits anomalous resonance if, as the loss goes to zero, the field magnitude diverges throughout a specific region (with sharp boundaries not defined by any discontinuities in the relative permittivity) but converges to a smooth field outside that region. Thus, cancelation of the fields at the polarizable dipoles shows up to avoid the infinite energies of the sources that would be otherwise present if the line dipoles were not cloaked. Also, Sec. 3 of Ref. [13] contains a rigorous proof that a finite number of interacting polarizable line dipoles at fixed positions will be cloaked in any arbitrary field, not just a linear one.

An early proposal to achieve invisibility of three-dimensional objects is due to Kerker [15],

who found that coated confocal ellipsoids could be invisible to long wavelength plane waves. Similar properties of transparency to electromagnetic waves for spheres, in the dipole limit, have been discussed by Alu and Engheta [16, 17]. A different approach, based on sensing and generating appropriate response fields at the boundary of the inclusions, has been suggested by Ramm [18] and Miller [19]. Reviews of this rapidly developing field may be found in articles by Sheng [20] and Weiss [21].

We will present here the results of numerical studies of the quasistatic electromagnetic cloaking for systems with cylindrical symmetry. While our simulations are limited to the two-dimensional quasistatic case, it has been shown that [13] a polarizable point dipole near a slab lens is cloaked and that this cloaking extends to the full time-harmonic Maxwell equations with a Veselago lens. Here, we will consider systems of polarizable line dipoles placed in an external field, and moving slowly in the vicinity of a coated cylinder. The coating material will be given a relative permittivity whose real part is the negative of that of the external region, and the region within it, and whose imaginary part is small and positive. We will show the first simulations illustrating the quenching of the induced moments on the polarizable line dipoles, as they move into the cloaking region surrounding the coated cylinder. The simulations will also clarify the cloaking mechanism, by illustrating the delicate reorganization of resonant fields on the cloaking cylinder which adjust themselves to place each polarizable molecule in the cloaking region at a point of near zero total electric field. The simulations show cloaking not only for polarizable lines with dipolar polarizability, but also for polarizable line with an isotropic quadrupolar response to the double gradient of the potential acting on it.

2. Theoretical considerations

The physical system considered here consists of a coated cylinder, which makes a hollow cylindrical perfect lens, and a set of N polarizable line dipoles placed at the points $P_1, P_2, \dots, P_j, \dots, P_N$, $P_j = (x_j, y_j)$, outside the cylinder. The coated cylinder has a core of radius r_c and a relative permittivity $\epsilon_c = 1$, and a shell of radius r_s and an almost lossless relative permittivity ϵ_s close to -1 . The medium outside the cylinder has a relative permittivity $\epsilon_m = 1$. An external electric field is applied to this system (see Fig. 1). Note that this is an electrostatic treatment of a quasistatic problem. By quasistatic we mean that the diameter of the coated cylinder is sufficiently small, and hence that the gradients of the fields are sufficiently large, that the spatial parts of the fields may be derived from the solution of the Laplace equation rather than the Helmholtz equation.

In the regions of the core, shell, and the annular region D of the matrix (exterior to the shell and extending as far as the nearest source), the complex potential is the solution of the Laplace equation. For example, in region D (see Fig. 1), it has the form [12, 13]

$$V(r, \theta) = A_0^e + \sum_{\ell=1}^{\infty} \left(A_{\ell}^e r^{\ell} + B_{\ell}^e r^{-\ell} \right) \cos(\ell\theta) + \left(A_{\ell}^o r^{\ell} + B_{\ell}^o r^{-\ell} \right) \sin(\ell\theta), \quad (1)$$

with similar forms applying within the shell and the core (excluding terms that are singular at the origin) [22]. Here, θ is measured from the x -axis. The superscripts 'e' and 'o' denote functions which are, respectively, symmetric and antisymmetric under the transformation $\theta \rightarrow -\theta$. Note that because ϵ_s is complex, the coefficients in (1) are also complex.

By means of the boundary conditions of continuity of the potential and the normal component of the electric flux density at the shell and core surfaces, the coefficients $B_{\ell}^{e/o}$ in Eq. (1) may be expressed in terms of A_0^e , A_{ℓ}^e , and A_{ℓ}^o .

We assume that each polarizable particle acquires a dipole moment proportional to the total electric field at the point where the particle is placed. Thus, in terms of electric potentials, at an



Fig. 1. A coated cylinder centered about the origin of coordinates. Polarizable line dipoles are placed at the points P_1, P_2, \dots, P_n . E_{appl} is an electric field with sources at infinity. The annular domain D , between the shell of the cylinder and the dashed circle, is chosen so that it contains no field sources. $P(z)$ is an arbitrary point in the plane where the total electric potential is evaluated.

arbitrary point z in the matrix and outside the cylindrical lens, the total complex potential has the form

$$V_m(z) = V_{\text{appl}}(z) + \sum_{n=1}^N V_n(z) + \tilde{V}_{\text{appl}}(z) + \sum_{n=1}^N \tilde{V}_n(z), \quad (2)$$

where $V_{\text{appl}}(z)$ is the potential of the external electric field, $V_n(z)$ is the potential of the induced dipole moment of particle n , $\tilde{V}_{\text{appl}}(z)$ represents the response of the cylindrical lens to the external field, and $\tilde{V}_n(z)$ represents the response of the cylindrical lens to the electric field of the n^{th} induced dipole moment. Note that when writing equation (2) we understand that, in fact, each term is expressed in terms of analytic functions of z and \bar{z} , as shown in [22].

In Cartesian coordinates, an induced dipole j is characterized by its moment $\mathbf{d}_j = (d_x^{(j)}, d_y^{(j)})$ which is given by the equation

$$\begin{bmatrix} d_x^{(j)} \\ d_y^{(j)} \end{bmatrix} = \alpha_j \begin{bmatrix} E_x^{(j)} \\ E_y^{(j)} \end{bmatrix} \equiv -\alpha_j \nabla \hat{V}^{(j)} \Big|_{z=z_j}, \quad (3)$$

in which α_j is the polarizability of the dipole, and

$$\hat{V}^{(j)} = V_{\text{appl}}(z) + \sum_{n \neq j} V_n(z) + \tilde{V}_{\text{appl}}(z) + \sum_{n=1}^N \tilde{V}_n(z) = V_m(z) - V_j(z). \quad (4)$$

Thus, the field at $z = z_j$ is due to the applied field, the response to it from the cylinder, fields coming from all other dipoles, and the response of the cylinder to all dipoles. Equations of the form (3) for all $j = 1, 2, \dots, N$ constitute a system of linear equations that we solve for the dipole moments [22]. Finally, with the dipole moments determined we can reconstruct the potential

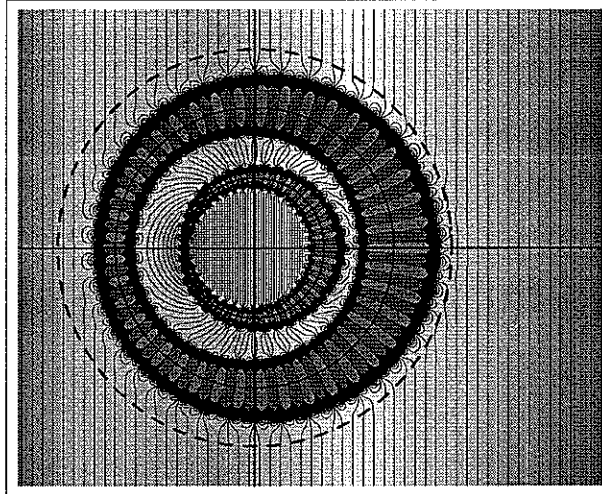


Fig. 2. Potential distribution showing cloaking of a single polarizable dipole ($\alpha = 2$, $E_{\text{appl}} = 1$, $\epsilon_m = \epsilon_c = 1$, $\epsilon_s = -1 + 10^{-12}i$, $r_s = 4$, $r_c = 2$, $r_{\#} = 5.66$, plot range = [-15 (blue), 15 (red)] for the potential). The concentric circles, shown in this and the following figures, bound the core (solid line), the shell (solid line), and the cloaking region (dashed line).

everywhere, inside and outside the cylindrical lens, using Eq. (2) and its extensions in the shell and core.

A key numerical parameter is the value chosen for the imaginary part of the relative permittivity of the shell material, $\text{Im}(\epsilon_s)$. This cannot be set equal to zero, since the problem of the interaction between the applied field, the polarizable line dipoles and the coated cylinder then has no convergent solution. However, it should be kept as small as possible, since otherwise the cloaking is much less distinct. In the results given here, we have chosen it to be typically 10^{-12} .

A difficulty arises when we work with systems of polarizable line dipoles (all with the same polarizability α) with their configuration such that a strong resonance occurs, which can mask the main features of the equipotential lines, and also the interaction with the cylindrical lens. (For an isolated pair of polarizable line dipoles this resonance occurs when α is the square of the interparticle distance). This difficulty is overcome by adjusting α to an appropriate value. (In movies 3 and 4 the value of α has been chosen anomalously large to make the cloaking effects more evident.)

The formulation was initially coded in *Mathematica* which, for small polarizable systems, is able to produce results of very high accuracy, even close to singular points. However, the computational efficiency was very poor and so we rewrote the code using the utility *MathLink* so as to perform all of the demanding numerical calculations in Fortran, employing *Mathematica* only to control the flow of operations and produce the final equipotential contour plots. Using this method the time required for simulations was decreased by up to a factor of approximately 100, making possible the animations of quite large systems of polarizable line dipoles discussed below. Using an Intel Pentium M processor of 1.86 GHz with Windows XP, the timing to obtain the contour plot in Fig. 6 (right panel), with 50,000 plot points for 26 line dipoles was 296

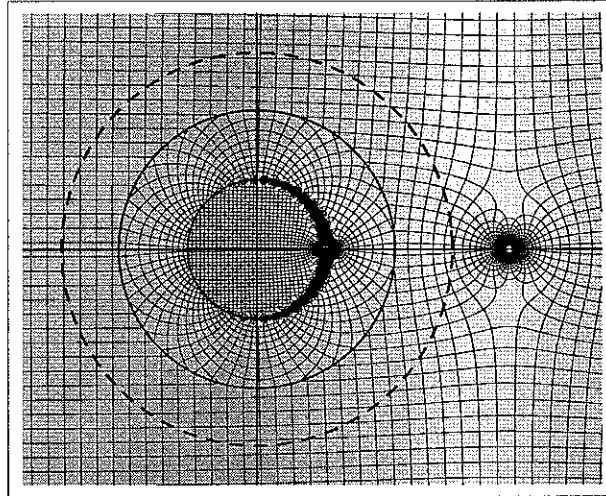


Fig. 3. The equipotential lines (generally vertical) and the electric field lines (generally horizontal) for a polarizable line dipole on the x-axis ($\alpha = 2$, $E_{\text{app}} = 1$, $\epsilon_m = \epsilon_c = 1$, $\epsilon_s = -1 + 10^{-12}i$, $r_s = 4$, $r_c = 2$, $r_{\#} = 5.7$, plot range = [-22 (blue), 25 (yellow)]).

seconds.

In the next section, we show in numerical simulations the real part of the complex potential. Since the physical potential is $\text{Re}(V \exp(-i\omega t))$ this means that we illustrate "snap-shots" of the physical potential at a subset of those times t_m such that $\omega t_m = 2m\pi$, for integer m .

3. Numerical simulations of cloaking

In some of the movies presented here we show the values of two parameters k_e and k_o [12, 13], which are related with the components of the dipole moment by the equation [22]

$$\begin{bmatrix} k_e^{(j)} \\ -k_o^{(j)} \end{bmatrix} = \begin{bmatrix} \cos \theta_j & \sin \theta_j \\ -\sin \theta_j & \cos \theta_j \end{bmatrix} \begin{bmatrix} d_x^{(j)} \\ d_y^{(j)} \end{bmatrix}, \quad (5)$$

where $\mathbf{d}^{(j)} = (d_x^{(j)}, d_y^{(j)})$ is the dipole moment of the dipole at $z_j = r_j \exp(i\theta_j)$.

Movie 1 (Fig.2) shows a single polarizable dipole moving towards the cloaking system. The boundary of the cloaking region is marked by the dashed circle of radius $r_{\#} = \sqrt{(r_s^3/r_c)}$ defined in Refs.[12, 13]. As the particle nears $r_{\#}$, we first see core-shell resonances, and then shell-matrix resonances, which rapidly quench the dipole moment of the particle (the resonant regions of alternating blue and red bands are where the potential is oscillatory and enormous, and has been truncated to avoid crowding of equipotential lines). Within the cloaking region $r < r_{\#}$, the resonances diminish, while the equipotential lines outside $r_{\#}$ are accurately those of the applied field alone. In Figs 3 and 4 we show the equipotential lines together with the electric field lines (Fig. 3) and the direction of the electric field (Fig. 4). Note the reversal of direction of electric field lines in Fig. 4 at the shell boundaries, a consequence of its negative

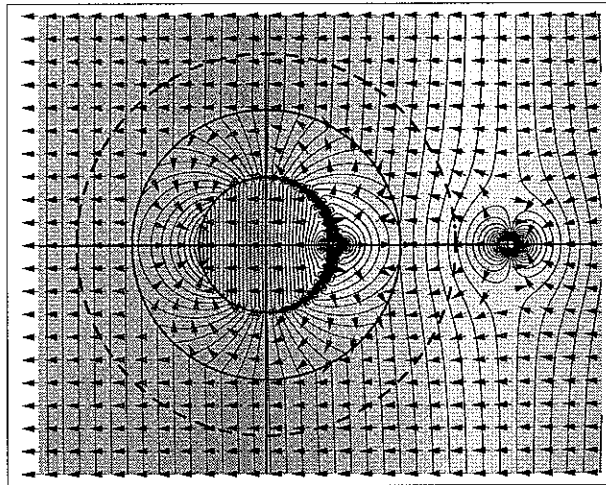


Fig. 4. The equipotential lines and the direction of the electric field (arrows) for a polarizable line dipole on the x-axis ($\alpha = 2$, $E_{\text{appl}} = 1$, $\epsilon_m = \epsilon_c = 1$, $\epsilon_s = -1 + 10^{-12}i$, $r_s = 4$, $r_c = 2$, $r_{\#} = 5.7$, plot range = [-22 (blue), 25 (red)]).

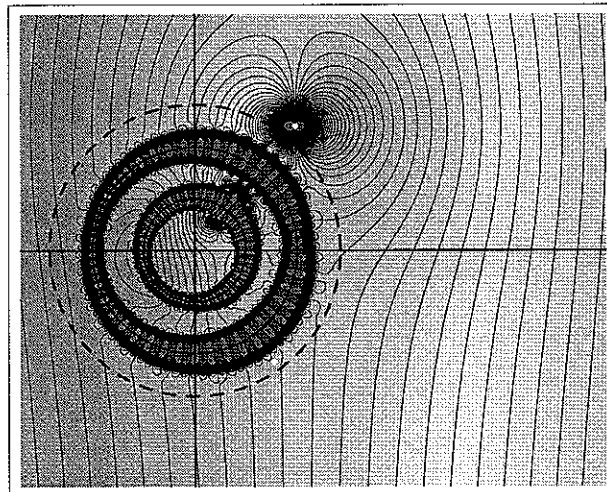


Fig. 5. Two polarizable dipoles, one cloaked and the other close to the cloaking region ($\alpha = 20$, $E_{\text{appl}} = 0.05$, $\epsilon_m = \epsilon_c = 1$, $\epsilon_s = -1 + 10^{-12}i$, $r_s = 4$, $r_c = 2$, $r_{\#} = 5.66$, plot range = [-2.5 (blue), 2.5 (red)]).

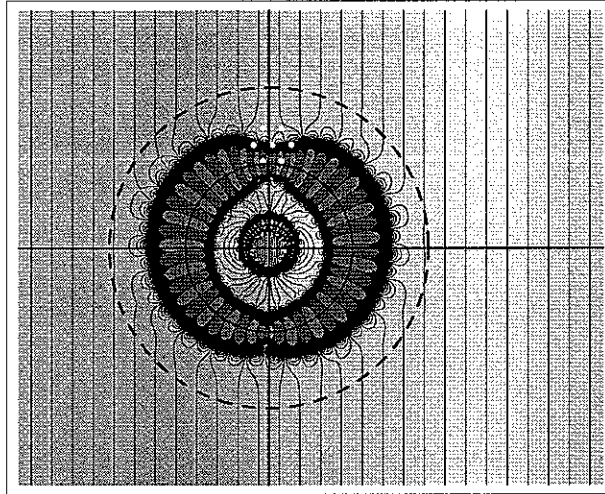


Fig. 6. Cloaking of a cluster of 7 polarizable dipoles in a hexagonal pattern ($\alpha = 20$, $E_{\text{appl}} = 0.05$, $\epsilon_m = \epsilon_c = 1$, $\epsilon_s = -1 + 10^{-12}i$, $r_s = 4$, $r_c = 1.1$, $r_{\#} = 7.63$, plot range = $[-2.5$ (blue), 2.5 (red)]).

relative permittivity, and also that the electric field lines in Fig. 3 are essentially equivalent to electric displacement field lines.

Movie 2 (Fig. 5) shows two identical polarizable dipoles moving parallel to the x axis. For $x \geq 0$ one polarizable dipole is always further to the left than the other.

Thus, the leftmost particle initiates resonant interactions first, and then is quenched, while the second is still outside $r_{\#}$. Note that when the leftmost particle is quenched, the other particle no longer interacts with it, but only with the cloaking cylinder, which however is effectively invisible to the other particle beyond the radius $r_{\#}$.

Movie 3 (Fig. 6) illustrates a cluster of seven polarizable line dipoles interacting with the cloaking system. One very interesting feature evident here is the rotation of the resonant lobes on the shell and core of the cloaking system, which continually realign themselves as the cluster moves. The essence of the cloaking interaction is that polarizable line dipoles which are being successfully cloaked must lie very close to saddle points of the potential. Exactly at such stationary points, the total field acting on them and their induced dipole moment would both be zero, but cloaking is never quite perfect: polarizable line dipoles sit near stationary points, so they have small dipole moments, and interact weakly with each other, and with the cloaking system. The equipotential lines outside $r_{\#}$ are quite close to those of the applied field when the cluster is deepest into the cloaking region (halfway through the movie).

Movie 4 (Fig. 7) shows both a single polarizable dipole and a system of 25 polarizable dipoles interacting with the cloaking system. The 25 dipoles are arranged around the silhouette of a shape from the popular cloaking literature, which is neither left-right or up-down symmetric. Very good cloaking is achieved for this quite complicated system. Note that the extended object perturbs the potential pattern much less than the particle when both are outside $r_{\#}$, and that

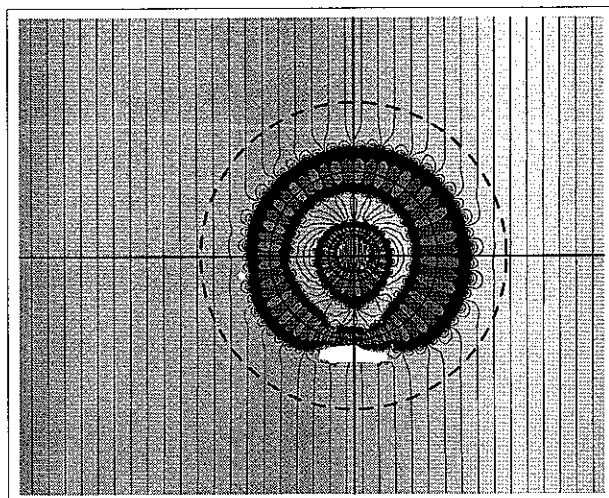


Fig. 7. Cloaking of a non-symmetric cluster of 25 polarizable dipoles plus one separate polarizable dipole ($\alpha = 20$, $E_{\text{appl}} = 0.05$, $\epsilon_m = \epsilon_c = 1$, $\epsilon_s = -1 + 10^{-12}i$, $r_s = 4$, $r_c = 1.2$, $r_{\#} = 7.3$, plot range = [-2 (blue), 2 (red)]).

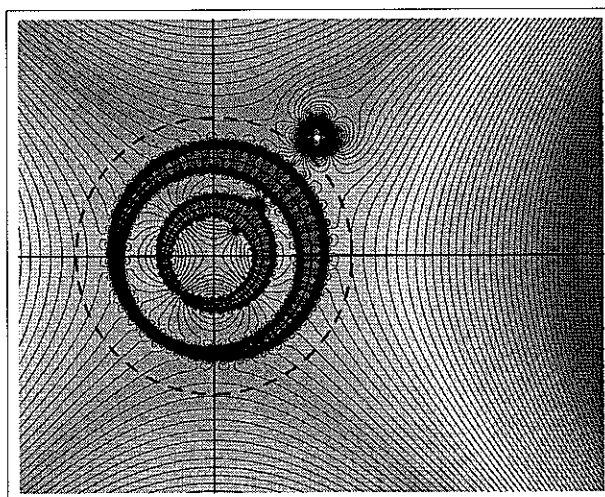


Fig. 8. A quadrupole close to the cloaking region ($\alpha = 20$, $E_{\text{appl}} = 0.05$, $\epsilon_m = \epsilon_c = 1$, $\epsilon_s = -1 + 10^{-12}i$, $r_s = 4$, $r_c = 2$, $r_{\#} = 5.66$, plot range = [-15 (blue), 15 (red)]).

the regions of most evident distortion are (not surprisingly) associated with regions of tightest curvature on the silhouette.

Movie 5 (Fig 8) shows the cloaking of a particle with a quadrupolar isotropic response to the double gradient of the voltage acting on it. Cloaking is achieved, and sets in quite quickly as the particle crosses the cloaking boundary $r = r_{\#}$.

4. Conclusion

The simulations we have given exemplify the complicated nature of the anomalous resonant interaction between the cloaking system of a metamaterial-coated cylinder and a system of polarizable line dipoles. Cloaking is achieved as the interaction between the system and the polarizable line dipoles rotates and adjust the resonant field pattern to follow the particle system. Note that for this to be possible, particle separation must be on the same or larger scale as the lobe pattern of the anomalous resonant system although the lobe pattern spacing does adapt itself somewhat to the particle separation. This latter is controlled by the imaginary part of the relative permittivity of the shell in a very sensitive way [12], so that the difficulty of translating these numerical results into an experimental realization should not be underestimated.

The support of the Australian Research Council and the National Science Foundation, through grant DMS-0411035, for this work is acknowledged, as are helpful communications from Prof. Oscar Bruno (see Ref. [23]) and Prof. Alexei Efros.